Easy Route to Superhydrophobic Copper-Based Wire-Guided Droplet Microfluidic Systems

Florian Mumm,* Antonius T. J. van Helvoort, and Pawel Sikorski*

Department of Physics, Norwegian University of Science and Technology, Høgskoleringen 5, Trondheim NO-7491, Norway

ARTICLE

ABSTRACT Droplet-based microfluidic systems are an expansion of the lab on a chip concept toward flexible, reconfigurable setups based on the modification and analysis of individual droplets. Superhydrophobic surfaces are one suitable candidate for the realization of droplet-based microfluidic systems as the high mobility of aqueous liquids on such surfaces offers possibilities to use novel or more efficient approaches to droplet movement. Here, copper-based superhydrophobic surfaces were produced either by the etching of polycrystalline copper samples along the grain boundaries using etchants common in the microelectronics industry, by electrodeposition of copper films with subsequent nanowire decoration based on thermal oxidization, or by a combination of both. The surfaces could be easily hydrophobized with thiol-modified fluorocarbons, after which the produced surfaces showed a water contact angle as high as 171° ± 2°. As copper was chosen as the base material, established patterning techniques adopted from printed circuit board fabrication could be used to fabricate macrostructures on the surfaces with the intention to confine the droplets and, thus, to reduce the system's sensitivity to tilting and vibrations. A simple droplet-based microfluidic chip with inlets, outlets, sample storage, and mixing areas was produced. Wire guidance, a relatively new actuation method applicable to aqueous liquids on superhydrophobic surfaces, was applied to move the droplets.

KEYWORDS: superhydrophobic surface · digital microfluidics · wire-guidance · CuO nanowires · printed circuit board

Superhydrophobic surfaces on which water droplets virtually form liquid balls are a well-known example of how design principles adopted from nature can be used in technology. Superhydrophobicity in nature is most prominently associated with the leaves of the lotus flower, where it is used as part of their cleaning mechanism.[1] The high water contact angle above 160° achieved by the leaves is due to their micro- and nanorough hydrophobic surface.[2] Both properties, a rough structure, which allows air to be trapped underneath the liquid, and a low surface energy, which makes the surface itself hydrophobic, are necessary for superhydrophobic surfaces with high mobility of water droplets.

Artificial superhydrophobic surfaces are generally produced by roughening or self-assembly of nonwetting materials or by fabrication of a micro- and/or nanorough surface followed by coating with a low surface energy layer. Using either of these methods, or a combination, a great variety of structures have been made.[3]

As the high apparent contact angle of water on superhydrophobic surfaces is a consequence of high surface roughness and low surface energy, nature's superior nanostructuring abilities can be counterbalanced in the fabrication of artificial surfaces by the use of nonbiological lower surface energy fluorocarbons instead of waxes.[4] Such artificial superhydrophobic surfaces or coatings are, among other things, investigated with respect to self-cleaning or corrosion protected interfaces, water repellent textiles or their applicability in droplet-based (or digital) microfluidic systems.[3,4]

In digital microfluidic devices, reactant solutions are confined as discrete droplets, which are then moved, mixed, and analyzed on the chip surface. Most research in the field is focused on devices either flowing two nonmixable phases through closed channels[5] or using actuation methods like electrowetting on dielectric (EWOD)[6] or dielectrophoresis[7] to individually move droplets on flat, conventionally hydrophobic electrode arrays. Droplet control on superhydrophobic surfaces could be achieved by using a magnetic field with droplets containing paramagnetic microparticles[8] or direct mechanical contact of the droplet to a guiding wire.[9] EWOD on superhydrophobic surfaces was demonstrated with water droplets[10] but failed in combination with biologically relevant buffer solutions.[11] Recently, reversible electrowetting on a silicon nanowire surface was shown as a new approach toward superhydrophobic EWOD systems.[12] Such systems are believed to be operable at lower voltages in comparison to traditional EWOD designs using flat interfaces.[13]

*Address correspondence to mumm@phys.ntnu.no, pawel.sikorski@phys.ntnu.no.

Received for review June 9, 2009 and accepted July 28, 2009.

Published online August 14, 2009.
10.1021/nn900607p CCC: $40.75

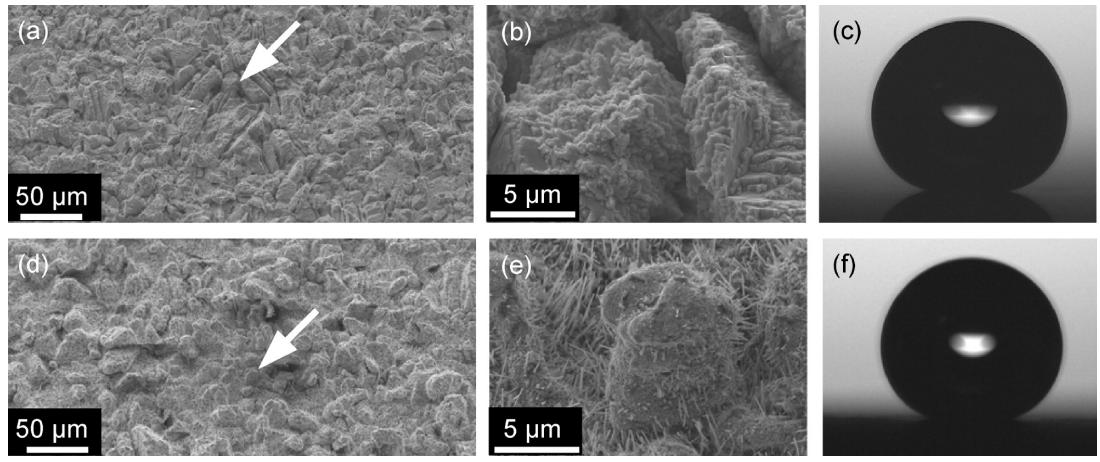

Figure 1. (Top) copper surface tilted by 45°: (a) overview, (b) closeup at the spot indicated by the arrow, (c) deposited water droplet. (Bottom) CuO surface after oxidization of the Cu surface tilted by 45°: (d) overview, (e) closeup at the spot indicated by the arrow, (f) deposited water droplet.

In contrast to other applications of superhydrophobicity, microfluidic systems are special in that they require the droplets to stay controllably on the surface. Consequently, the advantage of high droplet mobility connected to low roll-off angles comes at the expense of high sensitivity to tilting and vibrations. This sensitivity can be partially compensated with the introduction of structural features on the surfaces, which guide or confine the droplets.

Here we present a cheap and easy copper based approach, which allows controlled structuring from the millimeter length scale needed for droplet guidance of microliter-sized droplets down to the micro and nanometer length scales needed for superhydrophobicity. Copper is an omnipresent material in microelectronics, for example, as interconnects in integrated circuits or the base material for printed circuit boards (PCBs). Consequently, a diversity of copper patterning techniques for varying length scales have been developed.[14]

Copper-based surfaces are rather easily rendered superhydrohobic, and a huge variety of such systems have been published. This includes CuO microcabbages[15] and $Cu(OH)_2$ nanowires[16] created by solution-immersion, electrochemically fabricated Cu foams,[17] electroless galvanic deposition of silver or gold on Cu surfaces,[18] or etching. Etching was demonstrated using a modified Livingston's etchant,[19] or a potassium persulfate solution[20] on copper foils as well as a combination of nitric acid and hydrogen peroxide on copper alloys containing tin.[21]

Our approach is based on the etching of low grain size polycrystalline copper plates using cupric chloride, a standard etchant in the PCB industry,[22] or on electrodeposition of copper on copper foils. With both approaches macroscopic as well as microscopic structures can be produced. To further modify surface roughness and topography, both types of copper surfaces can be decorated with CuO nanowires by simple oxidization in air at elevated temperatures.[23]

RESULTS AND DISCUSSION

Surface Fabrication. Polycrystalline copper plates were used as the base material for surfaces made by etching (Figure 1a and b). Rough surfaces as well as dimples used for droplet confinement were created by etching through a resist mask using a solution of cupric chloride, hydrochloric acid, and water (see experimental methods). This was followed by subsequent mask removal using acetone and incubation in hydrochloric acid in an ultrasonic bath. In the etching step, unmasked copper is removed as cuprous chloride is formed from cupric chloride:[22]

$$CuCl_2 + Cu \rightarrow 2CuCl$$

CuCl is insoluble in pure water, so depending on the HCl concentration in the etchant, some of it may stick to the etched surface, forming a slightly green layer. During the final incubation in hydrochloric acid, these remains are dissolved owing to complex formation:[24]

$$CuCl + 3Cl^- \rightarrow [CuCl_4]^{3-}$$

As the droplet guiding patterns are comparatively broad (a 5 μL drop has a diameter of about 2 mm), a mask based on a conventional laser printer printout could be used.[25] An equivalent patterning approach has been recently presented for copper-based, flat, conventionally hydrophobic digital microfluidic devices.[26] After the first etching, mask removal, and cleaning in HCl, the process was repeated to achieve a similar surface topology at all parts of the chip (also those covered by the mask in the first etching step). As shown in Figure 1a,b, the surface roughness is caused by the shape and size of the copper grains exposed on the surface.

If intended, the roughness can be further modified by oxidizing the produced structures in air at 500 °C to allow for the spontaneous growth of CuO nanowires,[23] see Figure 1d,e. During the oxidation, a three layer system of Cu, Cu_2O, and CuO is formed.[27] Because of the

high surface mismatch between copper and its oxides, the oxide layer tends to flake off, so processing time, temperature, and heating and cooling steps have to be carefully controlled. This is especially important for large homogeneously nanowire covered surfaces.

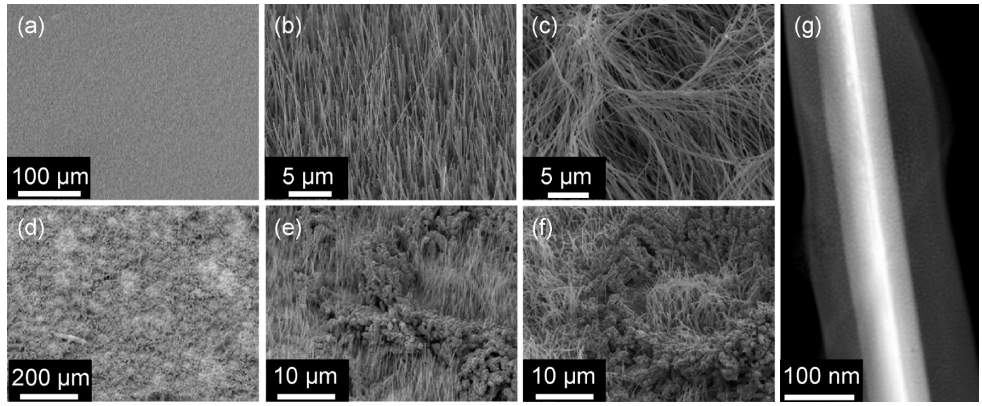

Figure 2. Surfaces created by thermal oxidization on electrodeposited substrates. (Top row) nanowire coated surface tilted by 45°: (a) overview, (b) closeup, (c) after incubation in HDFT. (Bottom row) 45° tilted view of nanowires on a surface with pores: (d) overview, (e) closeup, (f) after incubation in HDFT; (right) (g) high angle annular dark-field STEM image of a coated wire.

Surfaces based on electrodeposition (Figure 2) were produced in a two electrode electrolytic cell. An electrolyte based on $CuSO_4$ and H_2SO_4 in water was used to deposit a copper layer on copper foil. In the deposition process, macroscopic features might be fabricated by limiting the electrodeposition to areas not covered by a mask. Two types of surfaces were made: One consisting of a flat electrodeposited layer and the second consisting of a flat layer with pores deposited on top of it. Such porous layers can be produced by electrodeposition under a high potential, where the copper deposition at the cathode competes with hydrogen evolution. The emerging hydrogen bubbles act as temporary templates for the fabrication of porous copper structures.[28] These structures were themselves used to create superhydrophobic surfaces.[17] Both types of electrodeposited surfaces were then decorated with CuO nanowires by thermal oxidization. In the case of the flat surface, uniform growth of nanowires is observed, whereas for the porous surface nanowire growth is limited to the areas in and around the pores (Figure 2e,f). This is probably because the copper structures, which make up the pore walls, are too small to establish the Cu, Cu_2O, CuO layer needed for nanowire growth. Because of flaking of the oxide layer as described above, it proved to be difficult to fabricate a homogeneous nanowire layer on the cm^2 scale in a standard lab oven without control of the cooling process.

In a final step, the surface energy of all samples was reduced by incubation in a solution of fluorinated thiols (HDFT, see Experimental Methods). Thiols are known to form self-assembled layers on copper and cupric oxide either directly or because of the reduction of CuO to Cu or Cu_2O under disulfide formation.[29,30] For surfaces covered with nanowires, this process introduced a modification of the shape and orientation of the wires as can be seen in Figure 2. This is probably due to the partial reduction of CuO to Cu or surface-tension-induced bending. The main part of the nanowires remained nevertheless unreduced as CuO as confirmed by electron diffraction and electron energy loss spectroscopy data presented in the Supporting Information. An energy dispersive X-ray spectroscopy line scan across the wire depicted in Figure 2g showing a copper- and oxygen-containing core with a sulfur-containing layer around it is given in the Supporting Information as well.

Surface Characterization. Because of the simpler fabrication process, etching-based surfaces were used for fabrication of digital microfluidics test chips. Both the etched Cu and the etched and nanowire-decorated CuO surfaces showed similar high water contact angles of 171° ± 2° and 169° ± 2°, respectively, as shown in Figure 1c,f. As the presence of biomolecules tends to influence the contact angle, a cell culture medium (CellM: minimum essential medium with complements of fetal bovine serum, nonessential amino acids and L-glutamine, Invitrogen), a solution of 2 mg/mL BSA in water as well as 1 M Tris buffer (Sigma-Aldrich) and PBS (10 mM phosphate buffer, 2.7 mM potassium chloride, 137 mM sodium chloride, from tablets, Sigma-Aldrich) were additionally tested. The results are shown in Table 1. All of the solutions were movable by wire guidance as described below, both directly following the droplet deposition and after a 10 min waiting period.

Chip Components and Droplet Movement. Images of 7.5 μL droplets colored with food color on the structured surfaces are shown in 4. The figure shows a simple chip design consisting of an array of droplet confining dimples for the CuO surface as well as a slightly more complex layout for the Cu surface, where inlet and outlet holes were added. Droplet control on both surfaces could be

TABLE 1. Contact Angles for Different Solutions on the Surfaces Based on Etching[a]

	solution				
	water	Tris (1M)	PBS	CellM	BSA (2 mg/mL)
contact angle on Cu surface	171° ± 2°	169° ± 4°	170° ± 3°	166° ± 3°	168° ± 3°
contact angle on CuO surface	169° ± 2°	169° ± 2°	170° ± 2°	165° ± 1°	168° ± 3°

[a]Errors represent standard deviations based on six measurements on different positions.

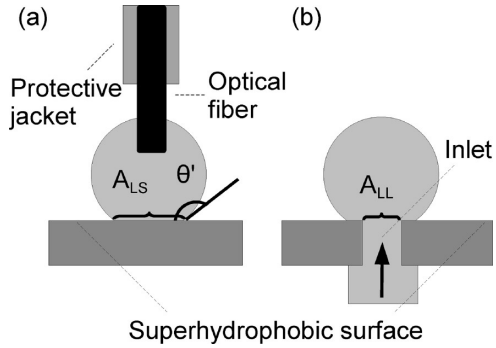

Figure 3. Principle of droplet motion (a) and inlet (b).

performed using a wire guidance approach with an optical fiber, which might be used as a readout device in future applications.

Wire guidance is based on the direct contact between the droplet and a guiding rod, either being moved manually or connected to a stage.[9] If the adhesion between the droplet and the rod is larger than between the droplet and the surface, the droplet follows the rod when it is moved.

The adhesion W_{adh} of a liquid to a surface is a function of the liquids surface tension γ_L as well as of its apparent contact angle θ' and the apparent interface area A_{LS} (see Figure 3a). It is given by the Young-Dupre equation:[9,31]

$$W_{adh} = \gamma_L(1 + \cos\theta')A_{LS} \quad (1)$$

Using 73 mJ/m^2 as the surface tension of water and a contact radius of about 0.75 mm as obtained experimentally for a 7.5 μL drop, and a contact angle of 170°, the adhesion to the surface can be calculated to about 2 nJ. The adhesion to an optical fiber used as a guiding rod depends on its material, its diameter, and the immersion depth into the droplet. For the fibers at hand, which were made of fused quartz, the water contact angle is known to depend on their chemical and thermal history.[32] To make sure that droplet guidance is possible, a comparatively high value of 30° is used in the calculations. With a fiber diameter of 250 μm (without the protective jacket) and an immersion depth of 1 mm, the adhesion can be calculated to 60 nJ. Consequently, the droplet is mobile on the surface when the fiber is moved. Achieving high contact angles is crucial for this approach.

For the Cu-based chip, a simple inlet and outlet design was adopted from Torkkeli:[11] Because of limited adhesion and weight, the deposition of droplets from the top becomes increasingly difficult with smaller volumes and higher contact angles.[33] In an alternative approach, loading can be conducted through a hole from the bottom as depicted in Figure 3b. For this purpose, 0.5 mm sized holes were drilled prior to the second etching step and subsequent hydrophobization. When the liquid is injected through the channel, it forms a droplet on the surface, which can be picked up by the fiber.

To detach the droplets from the inlet, the adhesion of the liquid to the fiber has to overcome the sum of the cohesion of the liquid W_{coh} and its adhesion to the surface W_{adh}. Approximating a flat separation interface between the droplet and the liquid in the hole, this can be calculated based on the apparent liquid−solid interface around the inlet $A_{LS'}$ and the central hole opening A_{LL}:[9]

$$W_{coh} + W_{adh} = 2\gamma_L A_{LL} + \gamma_L(1 + \cos\theta')A_{LS'} \quad (2)$$

Using a total contact radius of about 1 mm and a hole diameter of 0.5 mm, the total interfacial energy can be calculated to 32 nJ. The energy largely depends on the water/water contact area and can be further reduced by using smaller holes. As the adhesion to the fiber is larger than the combined adhesion and cohesion at the outlet, the droplet can be transferred onto the chip. Because of the comparatively large interaction with the fiber, bigger holes than demonstrated in EWOD systems could be employed.[11]

To inject the sample solutions, tubing was glued to the bottom side of the inlets and connected to syringes. The outlet was made by filling the holes with absorbing tissue paper from below. For additional confinement during storage and mixing, dimples are etched in the surface. In- and outlet holes are positioned in dimples as well (see Figure 4a). The chip proved to be functional and a short video of its manual operation showing repeating steps of droplet loading, droplet motion and mixing, and fiber washing is available as Supporting Information.

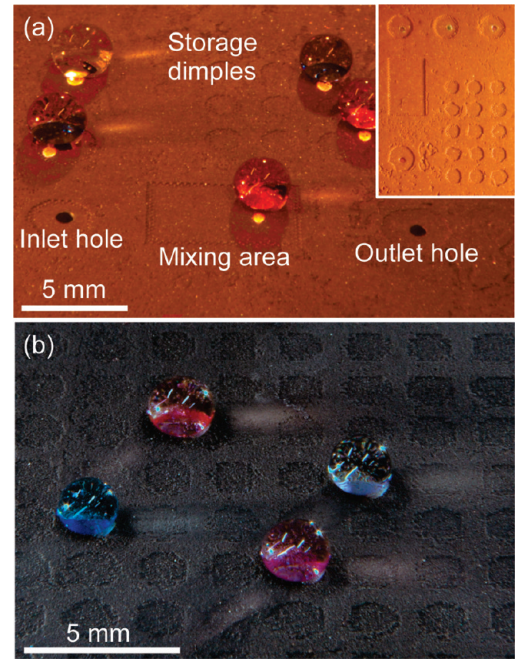

Figure 4. (a) Chip based on etched polycrystalline copper, inset showing chip layout; (b) Array of dimples on a surface made of nanowire decorated etched polycrystalline copper.

CONCLUSIONS

In conclusion, a simple approach to produce superhydrophobic surfaces mainly using polycrystalline copper samples and thiol chemistry has been presented. Using these surfaces in combination with developed structuring techniques from printed circuit board fabrication, a droplet-based superhydrophobic chip was produced and tested. The whole fabrication process consisting of etch mask deposition, etching, cleaning, and hydrophobic modification took less than 4 h and was feasible without specialized equipment. A water contact angle of 171° ± 2° was obtained. Further decoration of the surface with CuO nanowires by thermal oxidization was tested as an approach to further modify the surface roughness and resulted in an equally high water contact angle of 169° ± 2°. Wire guidance with an optical fiber was demonstrated as a suitable method for droplet movement on the patterned surfaces. For use in future applications, surface structuring, wire guidance, and possible readout from the optical fiber can be automated.

EXPERIMENTAL METHODS

Surface Fabrication. Polycrystalline 6 × 9 × 0.8 cm^3 large copper plates (Polymetaal, The Netherlands) were used as the base material for surfaces obtained by etching. The etching masks consisted of mirror images of the desired structures printed on transparencies using a standard laser printer with 1200 dpi resolution. The transparencies were placed on top of the plates, and the toner was transferred by heating to 200 °C under a load of about 5 kg. After 5 min, the plate was cooled down in a stream of water and the transparency could be detached while leaving the toner on the plate. Potential defects could be corrected with a water insoluble permanent marker. The plates were then etched in a solution of 25 g $CuCl_2$ and 25 mL HCl (37%) in 75 mL of water for 0.5 h followed by ultrasonification in 1 M HCl for several minutes. To change the surface morphology, CuO nanowires could be grown by oxidizing the samples in a preheated oven at 500 °C in air for 20 min. The samples were then cooled down on a heat resistant surface while covered with a Petri dish. As described earlier, flaking of the oxide layers from the copper base is a common problem in thermal growth of CuO nanowires, so a better control of this process is desirable. For the surfaces based on electrodeposition, copper foil was used as the substrate. To achieve a dense nanowire layer, Cu was deposited from an electrolyte containing 0.2 M $CuSO_4 \cdot 5H_2O$ and 1.5 M H_2SO_4 in water under a potential of 0.3 V in a two electrode electrolyte cell with a Cu counter-electrode for 45 min. The samples were then washed with 1 M HCl and water and dried under a nitrogen stream. Nanowire growth was obtained by incubation in a preheated oven at 500 °C in air for 45 min. To obtain a nanowire-coated porous surface, a second electrodeposition step was applied between deposition of the homogeneous Cu layer and thermal oxidization. In the second electrodeposition, a high potential of 10 V was used at a current density of about 1.5 A cm^{-1} for 10 s using a graphite rod as the counter electrode causing simultaneous Cu deposition and H_2 evolution. All samples were finally incubated in a 1 mM 1*H*,1*H*,2*H*,2*H*-perfluorodecanethiol (HDFT) solution in ethanol for 30 min followed by washing in ethanol for 30 min and repeated washing with ethanol thereafter.

Contact-Angle Measurements. Contact angles between the different solutions and the fabricated surfaces were determined using the sessile drop method and a KSV Instruments CAM 200 contact-angle meter.

Electron Microscopy. A Zeiss SUPRA 55 VP FESEM was used for scanning electron microscopy and a JEOL 2010F TEM for transmission and scanning transmission electron microscopy. The TEM was equipped with an INCA EDS system (Oxford Instruments) and a GIF 2000 energy filter (Gatan, Inc.).

Acknowledgment. The authors thank Dr. S. Volden (Department of Chemical Engineering, NTNU) for assistance with contact-angle measurements. F.M. acknowledges NTNU NanoLab for financial support.

Supporting Information Available: A video showing the manual operation of the droplet microfluidic chip shown in Figure 4a; analysis of the coated nanowires by transmission electron microscopy. This material is available free of charge *via* the Internet at http://pubs.acs.org.

REFERENCES AND NOTES

1. Barthlott, W.; Neinhuis, C. Purity of the Sacred Lotus, or Escape from Contamination in Biological Surfaces. *Planta* **1997**, *202*, 1–8.
2. Cheng, Y. T.; Rodak, D. E.; Wong, C. A.; Hayden, C. A. Effects of Micro-and Nano-Structures on the Self-Cleaning Behaviour of Lotus Leaves. *Nanotechnology* **2006**, *17*, 1359–1362.
3. Roach, P.; Shirtcliffe, N. J.; Newton, M. I. Progress in Superhydrophobic Surface Development. *Soft Matter* **2007**, *4*, 224–240.
4. Ma, M.; Hill, R. M. Superhydrophobic Surfaces. *Curr. Opin. Colloid Interface Sci.* **2006**, *11*, 193–202.
5. Huebner, A.; Sharma, S.; Srisa-Art, M.; Hollfelder, F.; Edel, J. B.; deMello, A. J. Microdroplets: A Sea of Applications. *Lab Chip* **2008**, *8*, 1244–1254.
6. Fair, R. B.; Khlystov, A.; Tailor, T. D.; Ivanov, V.; Evans, R. D.; Griffin, P. B.; Srinivasan, V.; Pamula, V. K.; Pollack, M. G.; Zhou, J. Chemical and Biological Applications of Digital-Microfluidic Devices. *IEEE Des. Test Comput.* **2007**, *24*, 10–24.
7. Schwartz, J. A.; Vykoukal, J. V.; Gascoyne, P. R. C. Droplet-Based Chemistry on a Programmable Micro-Chip. *Lab Chip* **2004**, *4*, 11–17.
8. Egatz-Gómez, A.; Schneider, J.; Aella, P.; Yang, D.; Domínguez-García, P.; Lindsay, S.; Picraux, S. T.; Rubio, M. A.; Melle, S.; Marquez, M.; *et al*. Silicon Nanowire and Polyethylene Superhydrophobic Surfaces for Discrete Magnetic Microfluidics. *Appl. Surf. Sci.* **2007**, *254*, 330–334.
9. Yoon, J.-Y.; You, D. J. Backscattering Particle Immunoassays in Wire-Guide Droplet Manipulations. *J. Biol. Eng.* **2008**, *2*, 15.
10. Torkkeli, A.; Saarilahti, J.; Haara, A.; Harma, H.; Soukka, T.; Tolonen, P. Electrostatic Transportation of Water Droplets on Superhydrophobic Surfaces. *Proc. IEEE MEMS 2001* **2001**, 475–478.
11. Torkkeli, A. Ph.D. Thesis. Helsinki University of Technology, 2003, ISBN 951-38-6238-0; http://lib.tkk.fi/Diss/2003/isbn9513862380/.
12. Verplanck, N.; Galopin, E.; Camart, J.-C.; Thomy, V.; Coffinier, Y.; Boukherroub, R. Reversible Electrowetting on Superhydrophobic Silicon Nanowires. *Nano Lett.* **2007**, *7*, 813–817.
13. Verplanck, N.; Coffinier, Y.; Thomy, V.; Boukherroub, R. Wettability Switching Techniques on Superhydrophobic Surfaces. *Nanoscale Res. Lett.* **2007**, *2*, 577–596.
14. Rickerby, J.; Steinke, J. H. G. Current Trends in Patterning with Copper. *Chem. Rev.* **2002**, *102*, 1525–1550.
15. Liu, J.; Huang, X.; Li, Y.; Li, Z.; Chi, Q.; Li, G. Formation of Hierarchical CuO Microcabbages as Stable Bionic Superhydrophobic Materials *via* a Room-Temperature Solution-Immersion Process. *Solid State Sci.* **2008**, *10*, 1568–1576.

16. Pan, Q.; Jin, H.; Wang, H. Fabrication of Superhydrophobic Surfaces on Interconnected $Cu(OH)_2$ Nanowires *via* Solution-Immersion. *Nanotechnology* **2007**, *18*, 355605.
17. Li, Y.; Jia, W.-Z.; Song, Y.-Y.; Xia, X. H. Superhydrophobicity of 3D Porous Copper Films Prepared Using the Hydrogen Bubble Dynamic Template. *Chem. Mater.* **2007**, *19*, 5758–5764.
18. Larmour, I. A.; Bell, S. E. J.; Saunders, G. C. Remarkably Simple Fabrication of Superhydrophobic Surfaces Using Electroless Galvanic Deposition. *Angew. Chem., Int. Ed.* **2007**, *46*, 1710–1712.
19. Qian, B.; Shen, Z. Fabrication of Superhydrophobic Surfaces by Dislocation−Selective Chemical Etching on Aluminum, Copper, and Zinc Substrates. *Langmuir* **2005**, *21*, 9007–9009.
20. Shirtcliffe, N. J.; McHale, G.; Newton, M. I.; Perry, C. C. Wetting and Wetting Transitions on Copper-Based Super-Hydrophobic Surfaces. *Langmuir* **2005**, *21*, 937–943.
21. Qu, M.; Zhang, B.; Song, S.; Chen, L.; Zhang, J.; Cao, X. Fabrication of Superhydrophobic Surfaces on Engineering Materials by a Solution-Immersion Process. *Adv. Funct. Mater.* **2007**, *17*, 593–596.
22. Cakir, O. Copper Etching with Cupric Chloride and Regeneration of Waste Etchant. *J. Mater. Process. Technol.* **2006**, *175*, 63–68.
23. Jiang, X.; Herricks, T.; Xia, Y. CuO Nanowires Can Be Synthesized by Heating Copper Substrates in Air. *Nano Lett.* **2002**, *2*, 1333–1338.
24. Cotton, F.; Wilkinson, G.; Murillo, C.; Bochmann, M. *Advanced Inorganic Chemistry,* 6th ed.; John Wiley & Sons, Inc.: New York, 1999; p 857.
25. Branson, J.; Naber, J.; Edelen, G. A Simplistic Printed Circuit Board Fabrication Process for Course Projects. *IEEE Trans. Educ.* **2000**, *43*, 257–261.
26. Abdelgawad, M.; Wheeler, A. R. Rapid Prototyping in Copper Substrates for Digital Microfluidics. *Adv. Mater.* **2007**, *19*, 133–137.
27. Hansen, B. J.; Lu, G.; Chen, J. Direct Oxidation Growth of CuO Nanowires from Copper-Containing Substrates. *J. Nanomater.* **2008**, Article ID 830474, published online, doi: 10.1155/2008/830474.
28. Shin, H.-C.; Dong, J.; Liu, M. Nanoporous Structures Prepared by an Electrochemical Deposition Process. *Adv. Mater.* **2003**, *15*, 1610–1614.
29. Keller, H.; Simak, P.; Schrepp, W.; Dembowski, J. Surface Chemistry of Thiols on Copper: An Efficient Way of Producing Multilayers. *Thin Solid Films* **1994**, *244*, 799–805.
30. Sung, M. M.; Sung, K.; Kim, C. G.; Lee, S. S.; Kim, Y. Self-Assembled Monolayers of Alkanethiols on Oxidized Copper Surfaces. *J. Phys. Chem. B* **2000**, *104*, 2273–2277.
31. Bangham, D. H.; Razouk, R. I. Adsorption and the Wettability of Solid Surfaces. *Trans. Faraday. Soc.* **1937**, *33*, 1459–1463.
32. Senn, B. C.; Pigram, P. J.; Liesegang, J. Surface Electrical Resistivity and Wettability Study of Fused Silica. *Surf. Interface Anal.* **1999**, *27*, 835–839.
33. Baret, J.-C.; Brinkmann, M. Wettability Control of Droplet Deposition and Detachment. *Phys. Rev. Lett.* **2006**, *96*, 146106.